Iterative Solution Methods for Coupled Vehicle-Structure Systems

Anna Feriani[1], Maria Gabriella Mulas[2]

[1]*DICATA, University of Brescia, Italy*
E-mail: *anna.feriani@ing.unibs.it*

[2]*Department of Structural Engineering, Politecnico di Milano, Italy*
E-mail: *mulas@stru.polimi.it*

SUMMARY. To solve the problem of vehicle-bridge dynamic interaction in time domain, the Authors proposed an uncoupled formulation of the equations of motion, that retains a sufficient generality in modelling the subsystems, and includes the effects of the pavement roughness. Based on this formulation, two iterative procedures were developed and coded, differing in the iteration scheme. The first one analyses separately the two sub-systems over the whole time history (WTH) and relies on a general purpose FE code for the structure. The second one analyses the two sub-systems at the same time and within the same code. Iteration is performed on each single time step (STS), according to a predictor-corrector scheme implemented in an *ad-hoc* code. Aim of this work is to investigate the stability properties of the iterative numerical methods, according to classical techniques: a general stability condition for procedure WTH is obtained, and then analysed more in detail for the case of a beam travelled by an oscillator. The analytical results obtained in the 2D case suggest the detection of an instability example for the 3D procedure, that is anyway outside of the range of interest of the model parameters. Preliminary studies show that the stability condition for procedure STS could present similar properties.

1 INTRODUCTION

The formulation of the equations of motion for the coupled system was derived in [1], under the following assumptions: (a) the bridge is modelled by a finite element model; (b) the vehicle moves at a constant horizontal velocity along a straight trajectory on the bridge; (c) the contact forces are vertical; (d) a bilateral point-wise contact is considered and (e) a constraint condition between the moving contact points and the nodes of the bridge mesh is imposed by making use of proper shape functions. The equations consider in a relatively simple way the pavement roughness and are not restricted to any particular modelling of both bridge and vehicle.

An uncoupled formulation of these equations was also proposed therein and two iterative procedures, were developed [1,2], differing in the numerical integration scheme. The first one analyses separately the two sub-systems over the whole time history (WTH) and relies on a general purpose FE code for the structure. The second one, that could be extended more easily to the case of non-linear subsystems, analyses the bridge and the vehicle conjointly within the same ad-hoc developed code. At each single time step (STS) a predictor-corrector scheme moves from vehicle to bridge and back to vehicle. A direct comparison of their performance in a selected case-study was presented in [2].

In the following, the coupled formulation and its uncoupling are briefly recalled in Section 2; the two iterative procedures are presented in Section 3. Section 4 describes the stability condition

for procedure WTH. Section 5 considers the case of an undamped beam travelled by an undamped oscillator and analyses its stability. Section 6 presents some numerical tests of the WTH procedure applied to a 3D model. A few conclusions are finally drawn.

2 THE EQUATIONS OF MOTION AND THEIR DECOUPLING

The coupled equations with reference to a FE discretisation were derived [1] for a vehicle travelling at constant speed c along a straight trajectory parallel to the bridge longitudinal axis, under the above mentioned assumptions. Since perfect contact is assumed between the vehicle and the bridge, the displacement and velocity of each contact point in the vehicle are written as a function of displacement, velocity and roughness at the corresponding point of the bridge. To this aim, the vector of the displacements and rotations of the bridge FE model is partitioned as $[q_b{}^T \, q_c{}^T]$, to separate the DOFs q_c of the nodes that will be directly loaded by the travelling vehicle from the remaining ones q_b. At the generic instant t, the contact points are not on a node of the bridge mesh and their displacements q_{cb} are determined as a function of q_c, making use of a proper shape function matrix N. A similar partitioning can be performed on the vehicle DOFs $[q_{cv}{}^T \, q_v{}^T]$ to separate the vertical displacements of the vehicle contact points q_{cv}, from the remaining DOFs q_v. At instant t the vehicle contact points occupy the positions $x(t)$ on the bridge, where the roughness profile has values $r(x(t))$. The constraint condition between vehicle and bridge, in terms of displacements, is thus written as:

$$q_{cv} = r(x(t)) + q_{cb} = r(x(t)) + N(x(t)) \, q_c(t) \tag{1}$$

Deriving (1) with respect to time, denoting with a dot the total time derivative and with a prime the spatial derivative, the vertical velocity of the vehicle contact points is:

$$\dot{q}_{cv} = \dot{r} + N\dot{q}_c + \dot{N}q_c \quad \text{with } \dot{N} = cN' \text{ and } \dot{r} = cr' \tag{2}$$

The Lagrange equations were adopted to derive the equations of motion [1]. To analyze the effect of the bridge static deflection on the interaction problem, the coordinates q of the coupled system are decomposed in the sum of two terms. The first one contains only the bridge static deflection q_0; the second contains the contribution q_d that includes the dynamic coupled response of both systems:

$$q = \begin{bmatrix} q_b \\ q_c \\ q_v \end{bmatrix} = \begin{bmatrix} q_{0b} \\ q_{0c} \\ 0 \end{bmatrix} + \begin{bmatrix} q_{db} \\ q_{dc} \\ q_v \end{bmatrix} = q_0 + q_d \tag{3}$$

Taking into account (3) the equations of motion can be written in terms of the coordinates q_d. To this aim the static deflection is considered through a modified roughness profile $r^* = Nq_{0c} + r$ and its time derivative $\dot{r}^* = \dot{N}q_{0c} + \dot{r}$. The equations of motion are written in compact form as:

$$M\ddot{q}_d + C\dot{q}_d + (K + K_c)q_d = Q_w(t) - Q_{r*}(t) - Q_{\dot{r}*}(t) \tag{4}$$

In (4) the matrices M, C and K of the coupled system are all symmetric, the mass matrix being time independent and the damping C and stiffness K matrices being time-dependent. The matrix K derives from the potential energy; K_c is an additional matrix, not symmetric and time dependent,

deriving from the vehicle dissipation function. K_c vanishes and a symmetric formulation is obtained when the tyre damping in the vehicle model is neglected or the third term in (2), containing the time derivative of the shape functions, is disregarded. At the RHS of (4), $Q_w(t)$ is the load vector due to the vehicle weight, while $Q_{r*}(t)$ and $Q_{\dot{r}*}(t)$ are the load vectors encompassing the effects of the pavement roughness, deriving from the potential energy and the dissipation function, respectively. The influence of wheel damping and the roughness effect, that is relevant, were analysed in [1] with reference to a given case study and to a roughness profile respecting Eurocode prescriptions [3].

The uncoupling of the equations takes advantage of the null terms in M, due to the absence of coupling in the inertial terms. To consider separately the two subsystems, the terms responsible for the lack of symmetry and for the time dependency of the matrices in (4) are moved to the RHS, since they contribute to the forcing vectors; adopting the same partition and index notation of (3) for the matrices in (4), the equations of motion can be written as:

$$
\begin{bmatrix} m_{b,b} & m_{b,c} & | & 0 \\ m_{b,c}^T & m_{c,c} & | & 0 \\ - & - & - & - \\ 0 & 0 & | & m_{v,v} \end{bmatrix} \begin{bmatrix} \ddot{q}_{db} \\ \ddot{q}_{dc} \\ - \\ \ddot{q}_v \end{bmatrix} + \begin{bmatrix} c_{b,b} & c_{b,c} & | & 0 \\ c_{b,c}^T & c_{c,c} & | & 0 \\ - & - & - & - \\ 0 & 0 & | & c_{v,v} \end{bmatrix} \begin{bmatrix} \dot{q}_{db} \\ \dot{q}_{dc} \\ - \\ \dot{q}_v \end{bmatrix} + \begin{bmatrix} k_{b,b} & k_{b,c} & | & 0 \\ k_{b,c}^T & k_{c,c} & | & 0 \\ - & - & - & - \\ 0 & 0 & | & k_{v,v} \end{bmatrix} \begin{bmatrix} q_{db} \\ q_{dc} \\ - \\ q_v \end{bmatrix} =
$$

$$
- \begin{bmatrix} 0 & 0 & | & 0 \\ 0 & N^T k_{cv,cv}^v N + N^T c_{cv,cv}^v \dot{N} & | & N^T k_{cv,v} \\ - & - & - & - \\ 0 & k_{cv,v}^T N + c_{cv,v}^T \dot{N} & | & 0 \end{bmatrix} \begin{bmatrix} q_{db} \\ q_{dc} \\ - \\ q_v \end{bmatrix} - \begin{bmatrix} 0 & 0 & | & 0 \\ 0 & N^T c_{cv,cv}^v N & | & N^T c_{cv,v} \\ - & - & - & - \\ 0 & c_{cv,v}^T N & | & 0 \end{bmatrix} \begin{bmatrix} \dot{q}_{db} \\ \dot{q}_{dc} \\ - \\ \dot{q}_v \end{bmatrix} + (5)
$$

$$
+ \begin{bmatrix} 0 \\ 0 \\ - \\ W_{0v} \end{bmatrix} - \begin{bmatrix} 0 \\ N^T k_{cv,cv}^v r* \\ - \\ k_{cv,v}^T r* \end{bmatrix} - \begin{bmatrix} 0 \\ N^T c_{cv,cv}^v \dot{r}* \\ - \\ c_{cv,v}^T \dot{r}* \end{bmatrix}
$$

3 THE ITERATIVE PROCEDURES WTH AND STS

A block Gauss-Seidel type of iteration is adopted to solve iteratively (5). Iterations are performed on the whole time history, as first proposed by Hawk and Ghali [4], in the WTH procedure and within the single time step in the STS procedure. As a preliminary step, both procedures consider the vehicle approaching the bridge on a rigid pavement having the prescribed roughness profile, to simulate the real situation. In fact, it was found in previous studies that the numerical solution is sensitive to the vehicle transient due to the initial conditions of motion.

For the WTH procedure each iteration is extended over the whole time history and is subdivided into four macro-steps, covering the determination of the forcing term and the numerical integration separately for the two systems. At the j-th iteration, at first the loading term for the vehicle is evaluated in (6a), considering the bridge displacements and velocities at the previous iteration; then the vehicle equations of motion are integrated in (6b); in (6c) the vehicle displacements and velocities determined in (6b) are used, together with the bridge displacements and velocities at the previous iteration, to determine the forces acting on the bridge and finally the bridge equations of motion are integrated in (6d):

$$f_v^{\ j} = -\left[k_{cv,v}^T\left(r*+Nq_{dc}^{j-1}\right)+c_{cv,v}^T\left(\dot{r}*+N\dot{q}_{dc}^{j-1}+\dot{N}q_{dc}^{j-1}\right)\right] \tag{6a}$$

$$m_{v,v}\ddot{q}_v^{\ j}+c_{v,v}\dot{q}_v^{\ j}+k_{v,v}q_v^{\ j}=W_{0v}+f_v^{\ j} \tag{6b}$$

$$P^j = N^T f^{\ j} = -N^T\left[k_{cv,cv}^v\left(r*+Nq_{dc}^{j-1}\right)+k_{cv,cv}q_v^j+c_{cv,cv}^v\left(\dot{r}*+N\dot{q}_{dc}^{j-1}+\dot{N}q_{dc}^{j-1}\right)+c_{cv,v}\dot{q}_v^j\right] \tag{6c}$$

$$\begin{bmatrix} m_{b,b} & m_{b,c} \\ m_{b,c}^T & m_{c,c} \end{bmatrix}\begin{bmatrix} \ddot{q}_{db}^{\ j} \\ \ddot{q}_{dc}^{\ j} \end{bmatrix}+\begin{bmatrix} c_{b,b} & c_{b,c} \\ c_{b,c}^T & c_{c,c} \end{bmatrix}\begin{bmatrix} \dot{q}_{db}^{\ j} \\ \dot{q}_{dc}^{\ j} \end{bmatrix}+\begin{bmatrix} k_{b,b} & k_{b,c} \\ k_{b,c}^T & k_{c,c} \end{bmatrix}\begin{bmatrix} q_{db}^{\ j} \\ q_{dc}^{\ j} \end{bmatrix}=\begin{bmatrix} 0 \\ P^j \end{bmatrix} \tag{6d}$$

At the first iteration the bridge is at rest, thus $q_{dc}^0=0$, $\dot{q}_{dc}^0=0$. It follows that the first approximation of vehicle motion in (6a,b) and contact forces in (6c) is obtained considering the vehicle travelling on a rigid uneven pavement having the prescribed roughness profile. Thus an estimate of the vehicle-bridge dynamic interaction is readily available by comparing the results at convergence with the ones obtained after the first iteration. Steps (6a) and (6c) are performed by interface programs. Step (6b) is performed by a specific vehicle module, adopting the trapezoidal rule for the direct integration; and step (6d) is performed by a multipurpose FE code.

At the end of step (6c), when $j>1$, for each wheel i a vector $R_i^{\ j}=f_i^{\ j}-f_i^{\ j-1}$ is assembled, having dimension equal to the number N_t of time steps covering the duration of the passage of the wheel on the bridge. The root mean square of the vector $R_i^{\ j}$ is assumed as a measure of the error on the i-th wheel. The iteration process ends when this quantity is smaller than a fraction λ, which is the tolerance specified in input, of the static load W_i acting on each wheel, that is:

$$err_i=\frac{1}{W_i}\sqrt{\frac{\sum_{l=1}^{N_t}\left(R_{i,l}^j\right)^2}{N_t}}\leq\lambda\ ;\quad i=1,n_{wheels} \tag{7}$$

If the criterion is not satisfied, the whole sequence (6a-d) is repeated.

In the STS procedure [2], the interaction between bridge and vehicle is analysed at each time step within the numerical integration process. If no iterations are performed, a staggered solution is obtained. At the beginning of the time step, the vehicle is moved to its final position. The nodal forces $P^{k,1}$ at step k, iteration 1, are obtained by keeping unchanged the wheel forces f^{k-1} at the end of previous step and applying them in the new location by updating the shape functions matrix N^k:

$$P^{k,1}=\left(N^k\right)^T f^{k-1} \tag{8}$$

With a proper modification of indices, the following steps can be deduced from (6a-d). The bridge response to these forces, computed as in (6d), is the prediction of the actual response. The vehicle forcing term is computed as in (6a); the vehicle equations are integrated as in (6b) and a corrected value of wheel forces $f^{k,1}$ is determined as in (6c). For the staggered solution, $f^{k,1}$ is the base for a new computation of (8) at the beginning of the following step, otherwise the unbalanced forces $\Delta f^{k,1}=(f^{k,1}-f^{k-1})$ are determined and iterations are performed. At the following iterations the

same steps are repeated adopting an incremental formulation.

The convergence check is always performed in finite form; for each wheel, the variation of the contact force in two subsequent iterations is determined, its ratio with respect to the static wheel load is calculated and averaged over the contact points. Such average is compared with a given tolerance.

4 A STABILITY CONDITION FOR PROCEDURE WTH

A classical stability condition for procedure WTH is sought, under the following assumptions: a) the bridge and vehicle equations are integrated with direct step by step methods considering the same time step, b) two algorithms of the Newmark family are adopted for the bridge and vehicle, which, in principle, could be different, with parameters γ_v, β_v and γ_p, β_p respectively, where $0\leq\gamma\leq1$ and $0\leq\beta\leq0.5$. The integration is performed in N_t time steps of duration Δt. At iteration j, vector X^j collects the state vectors $x^{n,j}$ of the whole time history:

$$\left(X^{j}\right)^{T} = \left[\left(x^{1,j}\right)^{T} \quad \left(x^{2,j}\right)^{T} \quad . \quad \left(x^{N_t,j}\right)^{T}\right] \tag{9}$$

where, at each time instant $t_n=n\Delta t$, the state vector $x^{n,j}$, which is more precisely a permutation of the state vector, is given by:

$$\left(x^{n,j}\right)^{T} = \left[\left(q_{db}^{n,j}\right)^{T} \quad \left(\dot{q}_{db}^{n,j}\right)^{T} \quad \left(q_{dc}^{n,j}\right)^{T} \quad \left(\dot{q}_{dc}^{n,j}\right)^{T} \quad \left(q_{v}^{n,j}\right)^{T} \quad \left(\dot{q}_{v}^{n,j}\right)^{T}\right] \tag{10a}$$

$$\left(x^{n,j}\right)^{T} = \left[\left(x_{b+c}^{n,j}\right)^{T} \quad \left(x_{v}^{n,j}\right)^{T}\right] \tag{10b}$$

In (10b), $x_v^{n,j}$ is the state vector of the vehicle. The state vector of the bridge $x_p^{n,j}$ is given by a permutation of the vector $x_{b+c}^{n,j}$:

$$\left(x_p^{n,j}\right)^{T} = \left[\left(q_{db}^{n,j}\right)^{T} \quad \left(q_{dc}^{n,j}\right)^{T} \quad \left(\dot{q}_{db}^{n,j}\right)^{T} \quad \left(\dot{q}_{dc}^{n,j}\right)^{T}\right]; \quad x_p^{n,j} = Px_{b+c}^{n,j} \tag{11a,b}$$

To obtain the iteration system, the step sequence (6a-d) is expressed first in matrix form as a function of the vectors $x_v^{n,j}$ and $x_{b+c}^{n,j}$. Within steps (6b) and (6d) the Newmark integration scheme is applied to the vehicle and the bridge. Then the relationships between the state vectors are assembled in order to find a relationship between the vectors X^j and X^{j-1}. As usual for stability analyses, the vectors containing known constant terms are dropped; thus the dependence on roughness disappears. After lengthy calculations [5], it is found that the iteration system:

$$SX^{j} = TX^{j-1} + const. \tag{12}$$

is characterized by lower block triangular (block bidiagonal) matrices S and T. With reference to partition (9), each subsystem of (12), relative to time t_n, can be written as:

$$-\left(\boldsymbol{D}_0 - \boldsymbol{E}^{n-1}\right)\boldsymbol{x}^{n-1,j} + \left(\boldsymbol{D}_1 - \boldsymbol{H}^n\right)\boldsymbol{x}^{n,j} = \boldsymbol{F}^{n-1}\boldsymbol{x}^{n-1,j-1} + \boldsymbol{G}^n\boldsymbol{x}^{n,j-1} \tag{13}$$

where matrices $\boldsymbol{E}, \boldsymbol{H}, \boldsymbol{F}, \boldsymbol{G}$, are described in detail in [5]. Superscripts n and n-1 denote that matrices are evaluated at times t_n and t_{n-1} respectively. Time dependency is related to the presence of the shape functions matrix $\boldsymbol{N}^n = \boldsymbol{N}(\boldsymbol{x}(t_n))$ defined in (1). Matrices $\boldsymbol{E}$ and $\boldsymbol{H}$ are block upper triangular with null sub-matrices on the main diagonal, while matrices $\boldsymbol{G}$ and $\boldsymbol{F}$ are block lower triangular. Matrices $\boldsymbol{D}_0$ and $\boldsymbol{D}_1$ are block diagonal, with each block related to the Newmark integration scheme of the relevant subsystem, that is:

$$\boldsymbol{D}_0 = \begin{bmatrix} \boldsymbol{D}_{0p}\boldsymbol{P} & \boldsymbol{0} \\ \boldsymbol{0} & \boldsymbol{D}_{0v} \end{bmatrix}; \qquad \boldsymbol{D}_1 = \begin{bmatrix} \boldsymbol{D}_{1p}\boldsymbol{P} & \boldsymbol{0} \\ \boldsymbol{0} & \boldsymbol{D}_{1v} \end{bmatrix} \tag{14a,b}$$

where the stability [6] of the two Newmark integration schemes adopted for the bridge and the vehicle depends on the properties of matrices $\boldsymbol{D}_{0p}, \boldsymbol{D}_{1p}$ and $\boldsymbol{D}_{0v}, \boldsymbol{D}_{1v}$, respectively:

$$\boldsymbol{D}_{1p}\boldsymbol{x}_p^{n,j} = \boldsymbol{D}_{0p}\boldsymbol{x}_p^{n-1,j} + \boldsymbol{B}_p\ ; \qquad \boldsymbol{D}_{1v}\boldsymbol{x}_p^{n,j} = \boldsymbol{D}_{0v}\boldsymbol{x}_v^{n-1,j} + \boldsymbol{B}_v \tag{15a,b}$$

In (15) vectors $\boldsymbol{B}_p$ and $\boldsymbol{B}_v$ are null in case of free oscillation. First of all, it is checked that the stability condition of the time integration schemes within iteration j, derived from (13), coincides with that obtained from (15a,b). According to (13), the time integration schemes within iteration j are stable if:

$$\rho(\boldsymbol{A}) = \rho\left(\left(\boldsymbol{D}_1 - \boldsymbol{H}^n\right)^{-1}\left(\boldsymbol{D}_0 - \boldsymbol{E}^{n-1}\right)\right) < 1\ ; n=1,..N_t \tag{16}$$

where ρ denotes the spectral radius. Since matrix $\boldsymbol{A}$ is block upper triangular and contains on the main block the diagonal matrices $(\boldsymbol{D}_{1p}\ \boldsymbol{P})^{-1}\ \boldsymbol{D}_{0p}\ \boldsymbol{P}$ and $(\boldsymbol{D}_{1v}\ )^{-1}\ \boldsymbol{D}_{0v}$ respectively, its stability condition reduces to the usual ones obtainable from (15a,b), that do not depend on n.

Then the stability of the block Gauss-Seidel scheme is investigated. The iteration matrix $\boldsymbol{S}^{-1}\ \boldsymbol{T}$ (12) is block triangular, with diagonal blocks equal to $(\boldsymbol{D}_1 - \boldsymbol{H}^n\ )^{-1}\boldsymbol{G}^n$, as it can be noticed using (13). Thus, the stability condition for the Gauss Seidel scheme, $\rho(\boldsymbol{S}^{-1}\ \boldsymbol{T}) < 1$, is equivalent to the conditions:

$$\rho\left(\left(\boldsymbol{D}_1 - \boldsymbol{H}^n\right)^{-1}\boldsymbol{G}^n\right) < 1\ ; \quad n=1,..N_t \tag{17}$$

If the wheel damping is not modelled or the third term in (2) is disregarded, the explicit dependence of the spectral radius on the vehicle velocity vanishes.

Equation (17) is obtained also, for implicit Newmark methods, when velocities and accelerations are expressed as a function of displacements and an iteration matrix is determined that relates displacements at iteration j to displacements at iteration j-1, as in steps (6a-d). In this case the stability conditions (16) are disregarded.

5 APPLICATION OF THE STABILITY CONDITION TO A BEAM

As a first check of the stability condition obtained in the previous Section, a simple case is analysed. An undamped beam, describing the bridge and discretised by beam finite elements, is

travelled by an undamped SDOF oscillator. In the 2D problem only transversal motion needs to be considered. The shape functions of the finite elements that are directly loaded are used. A consistent mass approach is adopted. In this case $x_{b+c}^{n,j} = x_p^{n,j} = x_c^{n,j}$, since all the beam coordinates belong to the subset "c". Assuming $\beta_p \neq 0$ the stability conditions (17), one for each time step, simplify in (see [5] for details):

$$\rho(\boldsymbol{M}^n) = \rho\left(-\alpha_v k_v \widetilde{\boldsymbol{\eta}}\left(\boldsymbol{N}^n\right)^T \boldsymbol{N}^n\right) < 1 \; ; \quad n=1,..N_t \qquad (18)$$

In (18) k_v is the oscillator stiffness; its natural circular frequency ω_v contributes to the factor $\alpha_v = 1/\left(1 + \beta_v \vartheta_v^2\right)$ through the parameter $\theta_v = \omega_v \Delta t$. Matrix $\widetilde{\boldsymbol{\eta}}^{-1} = \boldsymbol{m}_{cc} /\left(\beta_p \Delta t^2\right) + \boldsymbol{k}_{cc}$ is a combination of matrices $\boldsymbol{m}_{cc}$ and $\boldsymbol{k}_{cc}$, defined in (5), that in this simple case coincide with the beam mass and stiffness matrices, respectively. The stability of the Gauss-Seidel iteration does not depend on parameters γ_v and γ_p of the Newmark integration schemes.

Taking into account that in the case at study matrix $\boldsymbol{N}^n$ reduces to a row vector $(\boldsymbol{n}^n)^T$, it can be shown that matrix $\boldsymbol{M}^n$ has only one not null eigenvalue λ, which is real. Since matrices $\boldsymbol{m}_{cc}$ and $\boldsymbol{k}_{cc}$ are positive definite, $\lambda = \lambda_1$ is negative and the stability conditions (18) simplify in (19a):

$$\rho(\boldsymbol{M}^n) = -\lambda_1 = \alpha_v k_v \eta^n < 1 \; ; \quad n=1,..N_t \text{ with } \eta^n = \left(\boldsymbol{n}^n\right)^T \widetilde{\boldsymbol{\eta}} \boldsymbol{n}^n \leq \rho(\widetilde{\boldsymbol{\eta}})\left(\boldsymbol{n}^n\right)^T \boldsymbol{n}^n \qquad (19a,b)$$

The scalar η^n can be interpreted as a "flexibility coefficient" at the oscillator contact point, where the stiffness is incremented by the inertia effect. Considering the Rayleigh quotient properties, inequality (19b) follows.

The simplified stability analysis method recalled at the end of the previous Section, that assumes an implicit Newmark method and expresses velocities and accelerations as a function of displacements, was applied also to the STS procedure in finite form [5], and in this simple case the conditions (18) were again found, that are at least necessary.

5.1 *Beam discretised by Bernoulli beam elements: upper bound for the spectral radius*

The spectral radius of matrix $\boldsymbol{M}^n$ varies as the oscillator moves along the beam. If Bernoulli beam elements of length $h \leq \sqrt{6}$ are considered, it can be shown that $\left(\boldsymbol{n}^n\right)^T \boldsymbol{n}^n \leq 1$. Considering (19 a,b) it follows that:

$$\rho(\boldsymbol{M}^n) \leq \rho(\widetilde{\boldsymbol{M}}) \; ; \quad n=1,..N_t \quad \text{ with } \widetilde{\boldsymbol{M}} = -\alpha_v k_v \widetilde{\boldsymbol{\eta}} \qquad (20a,b)$$

Thus a sufficient condition for stability, that does not depend on n, is $\rho(\widetilde{\boldsymbol{M}}) \leq 1$.

5.2 *Simply supported beam: influence of stiffness parameters*

The simple case described in Section 5 is evaluated with respect to a simply supported beam, with linear density m, Young's modulus E, second moment of area J, length l, discretised by Bernoulli beam elements of length h.

The time integration step must be chosen small enough to integrate accurately both the oscillator motion and the beam motion and to model correctly the travelling load effect. To this purpose we can define: T_v the oscillator natural period; T_i the i-th beam natural period, and $\overline{T}_i$ the forcing period acting on the i-th vibration mode due to the travelling force effect, as:

$$T_v = \frac{2\pi}{\omega_v} \; ; \quad T_i = \frac{2l^2}{i^2\pi}\sqrt{\frac{m}{EJ}} \; ; \quad \overline{T}_i = \frac{2l}{ic} \tag{21 a,b,c}$$

It is reasonable to assume, in case of a smooth pavement, the following limitations:

$$\Delta t \leq \min\left\{\frac{T_v}{10}, \frac{T_i}{10}, \frac{\overline{T}_i}{10}\right\} \tag{22}$$

In the case of a SDOF oscillator representing a quarter car model travelling along a beam modelling a bridge, the mass and stiffness properties of the two subsystems and the vehicle speed c are such that $\overline{T}_i > T_i$. Having satisfied (22), it follows that $0.835 \leq \alpha_v = 1/\left(1 + \beta_v \vartheta_v^2\right) \leq 1$, where the lower limit rises up to 0.910 if the trapezoidal rule is adopted for the numerical integration of the vehicle motion. The factor α_v has thus little influence on the value of the spectral radius (19). Finally, the beam mass and stiffness matrices can be rewritten as:

$$\boldsymbol{m}_{cc} = \frac{hm}{420}\overline{\boldsymbol{m}}_{cc} \; ; \quad \boldsymbol{k}_{cc} = \frac{EJ}{h^3}\overline{\boldsymbol{k}}_{cc} \tag{23}$$

where, in the matrices $\overline{\boldsymbol{m}}_{cc}$ and $\overline{\boldsymbol{k}}_{cc}$, the elements that relate translational accelerations and displacements respectively to forces are dimensionless.

If $\Delta t = T_i/10$ is adopted, assuming $\beta_p = 0.25$ and taking into account (21b) and (23), a relation is obtained that, when included in (19), proves that the spectral radius is directly proportional to the ratio k_v/EJ:

$$\frac{1}{\beta_p \Delta t^2}\boldsymbol{m}_{cc} + \boldsymbol{k}_{cc} = i^4 \frac{5\pi^2}{21}\frac{h}{l}\frac{EJ}{l^3}\overline{\boldsymbol{m}}_{cc} + \frac{EJ}{h^3}\overline{\boldsymbol{k}}_{cc} \tag{24}$$

5.3 Simply supported beam: numerical results

The stability condition of the WTH procedure is analysed adopting the trapezoidal rule for both the oscillator and the beam. Since an unconditionally stable method is chosen for the time integration of both subsystems, only the stability condition of the iterative method is relevant. A simply supported beam with span $l=30.3$ m, linear density $m=22.615$ t m^{-1}, Young's modulus $E=2.94\text{x}10^7$ kPa, second moment of area $J=2.068$ m^4 is considered. A discretisation with 30 Bernoulli beam elements corresponds to the 2-D model of the bridge adopted in [1] for procedure STS. The SDOF oscillator stiffness $k_v=1.8\text{x}10^4$ kN m^{-1}, and mass $m_v=40$ t, are respectively equal to the sum of the suspensions stiffness and to the total mass of the 3D vehicle adopted in [2].

First of all, assuming $h=1.01$ m and considering a time step $\Delta t=0.001$ s, the spectral radius (19) is evaluated when the oscillator position coincides with a node of the FE model. The spectral radius is almost constant along the beam, increases less than 5% towards the beam ends and then decreases close to the supports. Further tests showed that the peak position slightly changes when the discretisation is varied.

For this reason in the following analyses the oscillator was placed at the node corresponding to

the centre of the span (position 1). A second position was chosen, that corresponds to the centre of the elements that are the closest ones to the midspan (position 2). The spectral radius (19) was compared with its upper bound (20). In Figure 1a, for a time step $\Delta t=0.001$ s the discretisation varies, adopting an even number of beam elements. In Figure 1b the ratio $h^2/\Delta t$ is constant, consistently with the Bernoulli beam wave propagation velocity for each bending mode; the space and time intervals are equal to $h=\lambda_k/8$ and $\Delta t=T_k/10$ respectively, being λ_k and T_k the wavelength and natural period of the k-th bending mode. With a constant time increment, the spectral radius at positions 1 and 2 tends to a constant value as h diminishes, as expected; the upper bound (20), that in this test holds also for $h>\sqrt{6}$, cannot catch such trend (Fig. 1a). If both Δt and h diminish consistently, the spectral radius decreases proportionally to Δt^α, with $\alpha\approx1.5$.
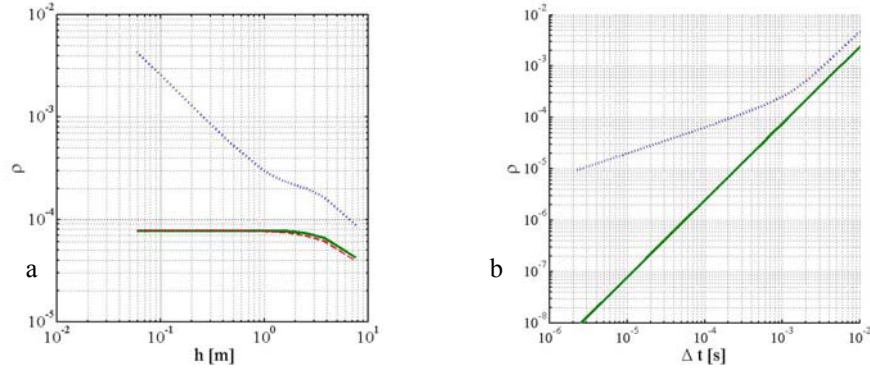
Figure 1: Spectral radius: a) vs h: upper bound, dotted; position 1, solid: position 2, dashed; b) vs Δt: upper bound, dotted; position 1, solid.

The time integration and discretisation parameters assumed in the analyses performed in [1] and [2] lead to a stable procedure in the 2D case. If a time increment $\Delta t=0.0003$ s is adopted, keeping the other parameters unchanged, to reach the stability limit the oscillator stiffness should be multiplied by a factor whose order of magnitude is 10^4.

6 NUMERICAL TESTS ON THE STABILITY CONDITION OF THE 3D MODEL

Numerical tests were performed on the 3D FE model of the same bridge, described in [1], in order to detect the stability limit of procedure WTH in this application. The upper slab is discretised by shell elements, and isoparametric shape functions are adopted to interpolate bridge displacements at the contact points and to determine the nodal equivalent forces. Masses are discretised by a lumped approach. The bridge motion (6d) is integrated by modal superposition.The vehicle is modelled by a 3D, 7-DOF lumped parameter model described in [2]; the rigid body modelling the sprung mass is connected to the four wheels of mass $m_{r,i}$ through a spring-damper system (of constants $k_{s,i}$, $c_{s,i}$) simulating the mechanical properties of the suspensions. The wheel masses are connected to the ground through another spring-damper system, reproducing the mechanical properties of the tyres (of constants $k_{r,i}$, $c_{r,i}$).

In the tests, $k_{r,i}=k_{s,i}=k$ is assumed, the roughness is present as a triggering factor and a vehicle speed equal to 30 ms^{-1} is considered. In order to perform a comparison with the 2D results, both bridge and vehicle damping are disregarded. A time increment $\Delta t=0.0003$ s is adopted for the bridge; the vehicle integration time step is equal to $\Delta t=0.000\overline{306}$.

Fig. 2 shows the error parameter err_i, defined in (7), for the front right wheel as a function of

the iteration number, for different values of k. A slow convergence is detected when k is equal to 5×10^5 kN m^{-1}; instability is detected when $k=5 \times 10^6$ kN m^{-1}. This result is one order of magnitude lower with respect to the 2D analytical case, but the agreement can be considered good, seen the differences in the two models. When an instability of the iterative procedure is detected, a stable case is obtained by decreasing the time increment, with the other parameters constant, as expected.
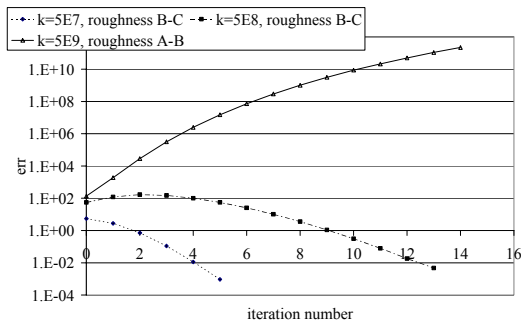
Figure 2: *err* at front right wheel vs iteration number

7 CONCLUSIONS

A general stability condition for procedure WTH is obtained, and then analysed more in detail for the case of a beam travelled by a SDOF oscillator. The analytical results obtained in the 2D case are in good agreement with numerical tests performed ad hoc on the 3D FE model. The stability condition for procedure STS could be investigated adopting the same method; a preliminary result is obtained. Both the analytical 2D and numerical 3D tests confirm that the range of interest of the model parameters is not prone to instability.

8 ACKNOWLEDGEMENTS

References
[1] Feriani A., Mulas M.G. and Lucchini G., "Vehicle-bridge interaction analysis: an uncoupled approach", in P. Sas, B. Bergen, editors, *Proc. of ISMA 2008*, 2008, Leuven, Belgium, 609-623.
[2] Feriani A. and Mulas M.G., "Numerical iterative analysis for vehicle-bridge dynamic interaction", in M. Pawelczyk and D. Bismor editors., *Recent Developments in Acoustic, Noise and Vibration, Proceedings of the 16th ICSV, on CD-ROM*, Krakow, Poland, 2009, 8 pp.
[3] Eurocode1, *Actions of structures. Part 2. Traffic loads on bridges*, EN1991-2, Annex B, 2003.
[4] Hawk H. and Ghali A., "Dynamic response of bridges to multiple track loading", *Canadian Journal of Civil Engineering*, **8**, 392-401 (1981).
[5] Rossini N., *Procedure iterative per l'analisi dell'interazione dinamica tra veicolo e ponte*, MS thesis, Università degli studi di Brescia, Facoltà di Ingegneria, A.A. 2007-08.
[6] Argyris J., Mlejnek H.P., "*Dynamics of Structures*", North Holland, 1991.